

A NEW SPECTRAL CLASSIFICATION SYSTEM FOR THE EARLIEST O STARS: DEFINITION OF TYPE O2

NOLAN R. WALBORN^{1,2}

Space Telescope Science Institute, 3700 San Martin Drive, Baltimore, MD 21218; walborn@stsci.edu

IAN D. HOWARTH³

Department of Physics and Astronomy, University College London, Gower Street, London WC1E 6BT, UK; idh@star.ucl.ac.uk

DANIEL J. LENNON⁴

Isaac Newton Group, Apartado 321, E-38700 Santa Cruz de La Palma, Canary Islands, Spain; djl@ing.iac.es

PHILIP MASSEY^{1,2} AND M. S. OEY¹

Lowell Observatory, 1400 West Mars Hill Road, Flagstaff, AZ 86001; massey@lowell.edu, oey@lowell.edu

ANTHONY F. J. MOFFAT¹ AND GWEN SKALKOWSKI

Département de Physique, Université de Montreal, C.P. 6128, Succ. Centre-Ville, Montreal, QC H3C 3J7, Canada; moffat@astro.umontreal.ca, gwen@astro.umontreal.ca

NIDIA I. MORRELL^{1,5}

Facultad de Ciencias Astronómicas y Geofísicas, Universidad Nacional de La Plata, Paseo del Bosque, 1900 La Plata, Argentina; nidia@fcaglp.fcaglp.unlp.edu.ar

LAURENT DRISSSEN²

Département de Physique, Université Laval, Ste-Foy, QC G1K 7P4, Canada; ldrissen@phy.ulaval.ca

AND

JOEL WM. PARKER¹

Southwest Research Institute, 1050 Walnut Street, Suite 426, Boulder, CO 80302; joel@boulder.swri.edu

Received 2001 September 18; accepted 2002 January 22

ABSTRACT

High-quality, blue-violet spectroscopic data are collected for 24 stars that have been classified as type O3 and that display the hallmark N iv and N v lines. A new member of the class is presented; it is the second known in the Cyg OB2 association, and only the second in the northern hemisphere. New digital data are also presented for several of the other stars. Although the data are inhomogeneous, the uniform plots by subcategory reveal some interesting new relationships. Several issues concerning the classification of the hottest O-type spectra are discussed, and new digital data are presented for the five original O3 dwarfs in the Carina Nebula, in which the N iv, N v features are very weak or absent. New spectral types O2 and O3.5 are introduced here as steps toward resolving these issues. The relationship between the derived absolute visual magnitudes and the spectroscopic luminosity classes of the O2–O3 stars shows more scatter than at later O types, at least partly because some overluminous dwarfs are unresolved multiple systems, and some close binary systems of relatively low luminosity and mass emulate O3 supergiant spectra. However, it also appears that the behavior of He II $\lambda 4686$, the primary luminosity criterion at later O types, responds to other phenomena in addition to luminosity at spectral types O2–O3. There is evidence that these spectral types may correspond to an immediate pre-WN phase, with a correspondingly large range of luminosities and masses. A complete census of spectra classified into the original O3 subcategories considered here (not including intermediate O3/WN types or O3 dwarfs without N iv, N v features) totals 45 stars; 34 of them belong to the Large Magellanic Cloud and 20 of the latter to 30 Doradus.

Key words: stars: early-type — stars: fundamental parameters

1. INTRODUCTION

Spectral class O3 was introduced by Walborn (1971a) to describe four stars in the Carina Nebula with earlier spectral types than the earliest (O4) MK standards. The initial spectroscopic criterion for the new class was the absence of He I $\lambda 4471$ in moderate-resolution (1 Å), widened photographic (IIa–O) spectrograms, whereas it is a well-defined, albeit weak, absorption line in O4 spectra. Three of the original O3 stars are of luminosity class V according to the criteria of Walborn (1971b, 1973a), with strong He II $\lambda 4686$ absorption, but one of them, HD 93129A, is the prototype of a qualitatively new kind of O-type spectra, displaying not only $\lambda 4686$ emission as in the Of supergiants, but also narrow N iv $\lambda 4058$ emission *stronger* than the normal Of N III

¹ Visiting or Staff Astronomer, Cerro Tololo Inter-American Observatory and/or Kitt Peak National Observatory, National Optical Astronomy Observatory, operated by the Association of Universities for Research in Astronomy, Inc., under cooperative agreement with the NSF.

² General Observer, *Hubble Space Telescope*, Space Telescope Science Institute, operated by the Association of Universities for Research in Astronomy, Inc., under NASA contract NAS 5-26555.

³ Visiting Observer, Isaac Newton Group, La Palma and Anglo-Australian Observatory, Siding Spring.

⁴ Visiting Observer, European Southern Observatory, La Silla.

⁵ Visiting Astronomer, Complejo Astronómico El Leoncito, operated under agreement of the Universidad Nacional de La Plata, the Universidad Nacional de Córdoba, the Universidad Nacional de San Juan, and the Consejo Nacional de Investigaciones Científicas y Técnicas de la República Argentina. Member of the Carrera del Investigador Científico, CONICET, Argentina.

$\lambda\lambda 4634, 4640\text{--}4642$ (denoted as f^*), and strong $N\ v\ \lambda\lambda 4604, 4620$ absorption lines. As also shown in the initial O3 paper, these $N\ iv$ and $N\ v$ features are weakly present in O4 If spectra, in particular with the $N\ iv$ emission weaker than the $N\ iii$; thus, a correlation between the absorption-line ($He\ ii/He\ i$) and selective emission-line (Walborn 2001) ionization ratios in these spectra was demonstrated. Two more O3 dwarfs in the Carina Nebula were added by Walborn (1973b), and HD 93129A was classified as O3 If*.

Subsequent quantitative analyses have demonstrated that the O3 stars are indeed the hottest representatives of Population I and the most massive (except for peculiar objects such as η Carinae and certain WNL stars, which are associated with the O3 stars in the Carina Nebula and are likely evolutionary descendants from them); furthermore, they have the most extreme stellar winds in terms of both ionization and terminal velocities (Kudritzki 1980; Simon et al. 1983; Kudritzki et al. 1992; Puls et al. 1996; Taresch et al. 1997; Haser et al. 1998; de Koter, Heap, & Hubeny 1998; Herrero, Puls, & Villamariz 2000; Herrero et al. 2001).

On the empirical side, the membership of the O3 class has grown steadily. An initial review by Walborn (1982) listed 10 members, all classified by the author, and presented the first members of subcategories O3 V(f^*), O3 III(f^*), and O3 If*/WN6-A. By the time of a second review (Walborn 1994), the class had grown to 27 definite and 43 possible members, through the work of a number of investigators. Since then, many additional O3 spectra have been found; they are scattered throughout the literature, so that a further review is now in order. Here we concentrate on a compilation of the pure O3 spectra that display the $N\ iv$ and $N\ v$ features, although the “adjacent” subcategories will also be discussed. In addition to a census, the objectives are to review (and possibly resolve) some outstanding issues in the spectral classification of these extreme stars, as well as their derived absolute magnitudes and masses.

2. DATA

The spectrograms displayed here are characterized by their resolution and signal-to-noise ratio (S/N) in the 10th and 11th columns of Table 1, respectively. Many of them have been published previously, and further information can be found in the references listed in the last column of the table. The remainder are presented here for the first time, and some further details about them are given below. It should be emphasized that all but one of the latter O3 stars have been previously classified as such in the literature, usually on the basis of earlier data; the corresponding references are given in the notes to the table.

The new O3 star announced here is Cyg OB2-22A. Cyg OB2-22 was classified O4 III(f) by Massey & Thompson (1991; their No. 417), but as further discussed later, this kind of spectrum can be produced by a composite of an O3 and a later OB type. Such has now been determined to be the case for Cyg OB2-22. Red spectroscopy was obtained by I. D. H. using the Intermediate Dispersion Spectrograph (IDS) at the 2.5 m Isaac Newton Telescope (INT) on 2000 July 20 and 21; it was immediately evident from the acquisition camera that the object is a visual double star. Follow-up blue-violet spectroscopy was obtained on 2000 August 11 with the Intermediate dispersion Spectroscopic and Imaging System (ISIS) spectrograph at the 4.2 m William

Herschel Telescope (WHT), through the Isaac Newton Group service program. For all observations, the spectrograph slit was aligned with the double-star components (the “B” component is estimated to be at P.A. = $150^\circ \pm 10^\circ$), and the spectrograms of the components were separately extracted by modeling the profile across the dispersion as the sum of two Gaussians of equal, but wavelength-dependent, width (an excellent approximation for these images). In this way the separation of the components was measured as $1''.55$ (with an uncertainty less than $0''.1$); for comparison, the spatial scale of the ISIS data is $0''.20\ \text{pixel}^{-1}$ with a point-spread function FWHM of $\sim 0''.9$, while the corresponding figures for the IDS data are $0''.33\ \text{pixel}^{-1}$ and $\sim 1''$. In both the blue and red data, the resolutions are $\sim 0.9\ \text{\AA}$ and the S/N 150–200 per wavelength point. The data yield relative magnitudes of $\Delta B = 0.33$ and $\Delta R = 0.40$; the difference is somewhat larger than the estimated uncertainties, but insufficient to provide compelling evidence for any difference in $B\text{--}R$ color between the components. We subsequently discovered that Pigulski & Kołaczowski (1998) found that Cyg OB2-22 “appeared to be a close double,” with $\Delta I = 0.37$. The composite blue-violet spectrogram of Cyg OB2-22AB shown later is derived from the spatially resolved WHT observation described above.

HD 64568 in NGC 2467/Puppis OB2 is the prototype of the O3 V(f^*) category (Walborn 1982), but no digital observation of its spectrum has been published. Such was kindly obtained for this project at the request of I. D. H. by K. C. Freeman at the Mount Stromlo/Siding Spring 2.3 m telescope on 2000 December 9–10. The total exposure time was 20 minutes. The resolution is $1.25\ \text{\AA}$ and the S/N is ~ 200 per wavelength point.

The sources of the other new data listed in Table 1 are as follows. Observations of stars in the Carina Nebula and N11/LH 10 in the Large Magellanic Cloud (LMC) were made by D. J. L. with the EMMI instrument at the New Technology Telescope of the European Southern Observatory, La Silla, during 1992 December 2–6; the resolution is $0.9\ \text{\AA}$ and the typical S/N is 100–200. The observation of LH 114-7 was obtained and discussed, but not reproduced, by Oey (1996; her designation D301SW-3); the instrument was the Argus multifiber spectrograph at the 4 m telescope of the Cerro Tololo Inter-American Observatory (CTIO). BI 253 was reobserved by P. M. with the CTIO 4 m RC spectrograph in 1999 January (see Massey et al. 1995; Massey, Waterhouse, & DeGioia-Eastwood 2000). The spectrogram of Sk $-71^\circ 51'$ was obtained by N. R. W. with the two-dimensional photon-counting system at the CTIO 1 m telescope on 1989 December 26–27; the observational parameters were as in Walborn & Fitzpatrick (1990), and a total exposure time of 3.3 hr yielded a maximum of 18,000 counts in the continuum, but substantial detector fixed pattern noise remains in this spectrogram despite efforts to reduce it during the observations. The new data for P871, P1163, and P1311 (Parker 1993) in 30 Doradus are from an Argus program led by A. F. J. M., with three runs during 1993–1996 involving multiple exposures to detect spectroscopic binaries, currently being analyzed; the spectrograms shown here are sums of the available exposures (no velocity shifts being detected in these cases), with a resolution of $\sim 2\ \text{\AA}$ and typical S/N of 150–200. Finally, additional, high-resolution observations of the Carina Nebula dwarfs were obtained by N. I. M. and N. R. W. with the Bench-Mounted Echelle spectrograph at the CTIO 1.5 m telescope during 1992

TABLE 1
STELLAR AND OBSERVATIONAL DATA FOR THE SPECTRA ILLUSTRATED

Star	R.A. (2000.0)	Decl. (2000.0)	V	$B-V$	Association	V_0-M_V	M_V	M/M_\odot	Resolution (\AA)	S/N	Source
O2–O3.5 If* (Fig. 3)											
HD 93129A.....	10 43 57.5	−59 32 53	7.3	0.22	Carina Nebula	12.2	−6.5	127/127	0.9	200	This paper
Cyg OB2-7.....	20 33 14.2	41 20 19	10.55	1.45	VI Cygni	11.3	−6.6	139/135	1.9	200	Walborn & Howarth (2000)
Cyg OB2-22A.....	20 33 08.9	41 13 15	12.12	2.04	VI Cygni	11.3	−7.3	266/200	0.9	200	This paper
Pismis 24-1.....	17 24 43.4	−34 11 56	10.43	1.45	NGC 6357	12.0	−7.4	291/210	1.8	80	Massey et al. (2001)
MACHO 05:34–69:31 ...	5 34 41.3	−69 31 39	13.69	−0.06	LMC	18.6	−5.7	61/82	3.6	100	Ostrov (2001)
MH 36.....	5 38 42.8	−69 06 03	14.49	0.06	30 Doradus	18.6	−5.2	38/66	3	60	Massey & Hunter (1998)
O2–O3.5 III(f*) with He II λ 4686 P Cygni Profile (Fig. 4)											
Sk −68°137.....	5 38 24.8	−68 52 33	13.26	−0.07	30 Doradus?	18.6	−6.1	101/99	0.5	70	Walborn et al. (1995)
LH 64-16.....	5 28 47.0	−68 47 48	13.62	−0.17	W16-8	18.6	−5.4	53/72	1	160	Massey et al. (2000)
LH 114-7.....	5 43 12.9	−67 51 16	13.66	−0.25	N70	18.6	−5.2	44/66	2.2	80	This paper
Pismis 24-17.....	17 24 44.7	−34 12 02	11.84	1.49	NGC 6357	12.0	−6.1	101/101	1.8	80	Massey et al. (2001)
LH 10-3209A.....	4 56 59.0	−66 24 38	12.73	−0.07	N11B	18.6	−6.6	160/140	3	60	Walborn et al. (1999)
HST-42.....	11 15 07.2	−61 15 39	12.86	1.12	NGC 3603	14.2	−6.0	92/95	3	60	Drissen et al. (1995)
HST-A3.....	11 15 07.5	−61 15 38	12.95	1.12	NGC 3603	14.2	−5.9	84/91	3	60	Drissen et al. (1995)
O2 III(f*) without He II λ 4686 P Cygni Profile (Fig. 5)											
HDE 269810.....	5 35 13.9	−67 33 27	12.28	−0.23	NGC 2029	18.6	−6.6	160/140	0.5	100	Walborn et al. (1995)
LH 10-3061.....	4 56 42.5	−66 25 18	13.68	−0.01	N11B	18.6	−5.8	77/85	0.9	100	This paper
NGC 346-3.....	0 59 01.1	−72 10 28	13.50	−0.23	NGC 346	19.1	−5.9	84/81	0.16	140	Walborn et al. (2000)
O2–O3 III(f*) + OB (Fig. 5)											
Sk −66°172.....	5 37 05.6	−66 21 36	13.13	−0.12	N64	18.6	−6.1	101/94	0.5	50	Walborn et al. (1995)
Cyg OB2-22AB.....	20 33 08.9	41 13 15	11.55	2.04	VI Cygni	11.3	−7.8	...	0.9	200	This paper
LH 10-3209.....	4 56 59.0	−66 24 38	12.66	−0.11	N11B	18.6	−6.6	...	3.4	90	Parker et al. (1992)
O2–O3 V((f*)) (Fig. 6)											
BI 253.....	5 37 34.3	−69 01 11	13.88	−0.13	30 Doradus?	18.6	−5.3	56/69	1	160	This paper
HD 64568.....	7 53 38.2	−26 13 57	9.39	0.11	NGC 2467	13.2	−5.1	46/63	1.25	200	This paper
LH 10-3058.....	4 56 42.2	−66 24 54	14.24	−0.06	N11B	18.6	−5.1	46/63	0.9	100	This paper
Sk −71°51.....	5 41 39.6	−71 19 56	12.71	−0.09	NGC 2103	18.6	−6.6	...	1.5	80	This paper
P871.....	5 38 41.6	−69 05 19	13.24	0.05	30 Doradus	18.6	−6.5	168/130	2.2	180	This paper
P1163.....	5 38 44.7	−69 04 50	13.96	−0.04	30 Doradus	18.6	−5.5	67/75	2.2	180	This paper
P1311.....	5 38 46.2	−69 06 16	13.80	0.08	30 Doradus	18.6	−6.0	106/94	2.2	180	This paper
O3.5–O5 V((f)) (Figs. 7 and 8)											
HD 93128.....	10 43 54.4	−59 32 58	8.77	0.24	Carina Nebula	12.2	−5.1	46/56	0.9	200	This paper
									0.26	130	This paper
HD 93129B.....	10 43 57.8	−59 32 55	8.9	0.22	Carina Nebula	12.2	−4.9	38/53	0.26	130	This paper
HD 93205.....	10 44 33.8	−59 44 16	7.75	0.05	Carina Nebula	12.2	−5.6	73/69	0.9	200	This paper
HD 93250.....	10 44 45.1	−59 33 55	7.38	0.15	Carina Nebula	12.2	−6.2	127/91	0.9	200	This paper
									0.26	130	This paper
HDE 303308.....	10 45 06.0	−59 40 06	8.17	0.13	Carina Nebula	12.2	−5.4	60/63	0.9	200	This paper
									0.26	130	This paper
HD 93204.....	10 44 32.4	−59 44 31	8.42	0.10	Carina Nebula	12.2	−5.0	43/55	0.9	100	This paper
HD 46223.....	6 32 09.3	4 49 24	7.25	0.22	NGC 2244	10.5	−5.4	60/63	0.26	130	This paper
HD 46150.....	6 31 55.5	4 56 34	6.72 _v	0.13	NGC 2244	10.5	−5.6	75/69	0.26	130	This paper

NOTE.—Units of right ascension are hours, minutes, and seconds, and units of declination are degrees, arcminutes, and arcseconds.

REFERENCES.—HD 93129A: Walborn 1971a, 1973b, 1974; Conti, Niemela, & Walborn 1979; Simon et al. 1983; Taresch et al. 1997. Cyg OB2-7: Walborn 1973c; Herrero et al. 2000, 2001. Pismis 24: Lortet, Testor, & Niemela 1984; Vijapurkar & Drilling 1993 (LSS 4142). Sk −68°137: Garmany & Walborn 1987; Haser et al. 1998. LH 114-7: Massey et al. 1995 (lmc2-675); Oey 1996 (D301SW-3). HDE 269810: Walborn 1977, 1982; Puls et al. 1996. LH 10: Parker et al. 1992; Walborn & Parker 1992. NGC 346-3: Walborn & Blades 1986; Niemela et al. 1986; Kudritzki et al. 1989; Walborn et al. 1995; Haser et al. 1998. BI 253: Massey et al. 1995. HD 64568: Walborn 1982. Sk −71°51: Garmany & Walborn 1987; Walborn 1994. P871, P1163, P1311: Melnick 1985; Parker 1993; Walborn & Blades 1997. Carina dwarfs: Walborn 1971a, 1973b, 1995; Conti & Walborn 1976; Kudritzki 1980; Simon et al. 1983; Puls et al. 1996; Morrell et al. 2001.

March 19–22; the 2 pixel resolution of these data is 0.26 \AA , and the S/N ranges between 100 and 150.

3. RESULTS

3.1. *Cyg OB2-22*

Figures 1 and 2 present the blue and red, respectively, spatially resolved spectra of *Cyg OB2-22A* and *B*, compared with the spectrum of *Cyg OB2-7*, O3 If*, as discussed by Walborn & Howarth (2000). As already mentioned, the combined light of No. 22AB was reasonably classified as O4 III(f) by Massey & Thompson (1991), and it was analyzed as such by Herrero et al. (1999). However, the spatially resolved spectrum of No. 22A shows no trace of He I lines, so it is of pure O3 type, here also classified as O3 If* for reasons that will become apparent later, although He II $\lambda 4686$ emission is somewhat weaker and the line has a clearer P Cygni profile than in No. 7. The He I lines in the combined light of No. 22 originate in the B component, which has a well-defined spectral type of O6 V((f)). Some other cases of O3 spectra with strong He I lines that have been resolved

into multiple systems will be noted below, and this general classification issue will be discussed further. As shown in Figure 2, the peculiar $H\alpha$ profiles of No. 7 and No. 22A are remarkably similar. Thus, *Cyg OB2-22A* becomes the second O3 supergiant in that association and only the second O3 star of any kind known in the northern hemisphere.

3.2. *The (Former) O3 Class*

Observational and derived data for the stars to be discussed are listed in Table 1, in the order in which their spectra are presented in Figures 3–8. The emphasis is on normal supergiants and giants with the best available data, with the addition of dwarfs showing the N IV, N V lines, and the original Carina Nebula O3 dwarfs in which those lines are weak or absent. Successive columns of Table 1 give the stellar designation, coordinates for equinox 2000.0, V and $B-V$,⁶ stellar or nebular association, distance modulus $V_0 - M_V$,

⁶ The magnitude of *Cyg OB2-22A* has been calculated from the combined light with the assumptions of the same color for both components and $\Delta V = 0.4$.

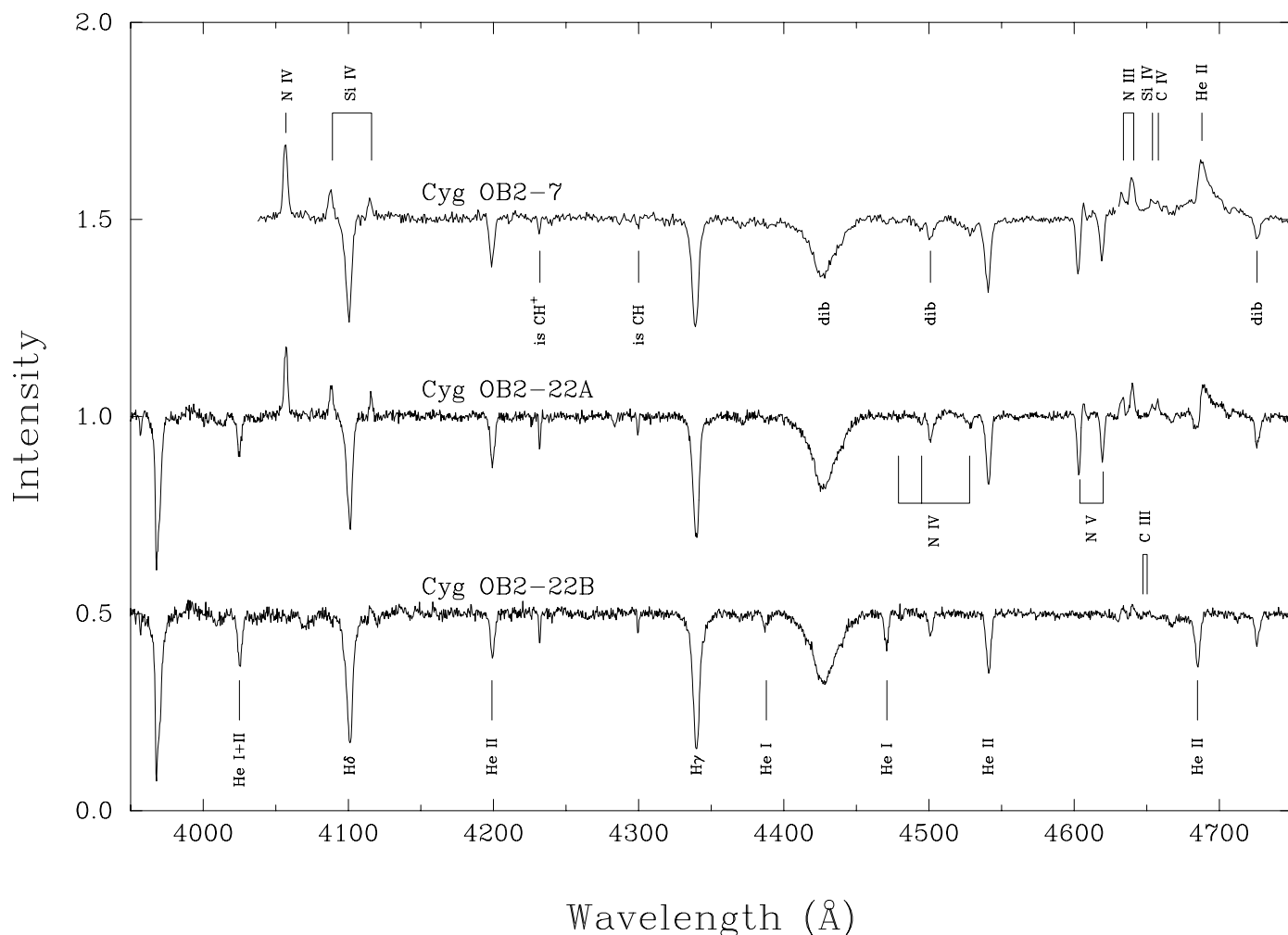


FIG. 1.—Rectified linear-intensity, blue-violet spectrograms of the spatially resolved components of *Cyg OB2-22*, with *Cyg OB2-7* for comparison. The stellar features identified above the spectrum of No. 7 are N IV $\lambda 4058$; Si IV $\lambda\lambda 4089-4116, 4654$; N III $\lambda\lambda 4634-4640-4642$; C IV $\lambda 4658$; and He II $\lambda 4686$; the wavelengths of the interstellar lines and diffuse interstellar bands identified below are given by Walborn & Howarth (2000). The lines identified in *Cyg OB2-22A* are N IV $\lambda\lambda 4478-4496-4530$ and N V $\lambda\lambda 4604-4620$; in *Cyg OB2-22B* they are He I $\lambda\lambda 4026 (+II), 4387, 4471$; H δ $\lambda 4102$; H γ $\lambda 4340$; He II $\lambda\lambda 4200, 4541, 4686$; and (above) the C III $\lambda 4650$ blend.

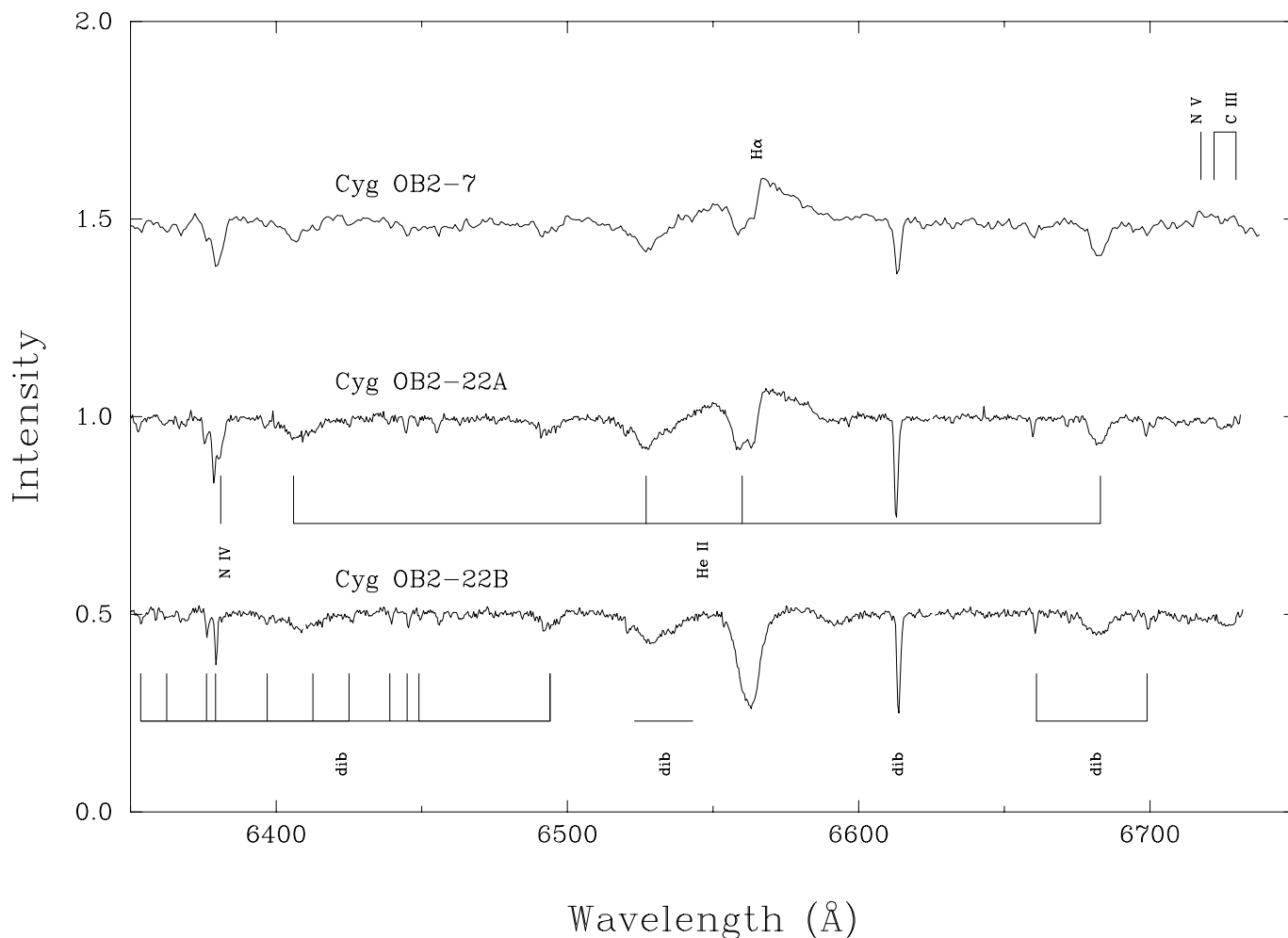


FIG. 2.—Red spectrograms of the Cyg OB2-22 components and Cyg OB2-7. The features identified in the spectrum of No. 7 are H α λ 6563; N v λ 6716–6718; and C III λ 6721, 6727–6731. In Cyg OB2-22A, the lines identified are N IV λ 6381 and He II λ 6406–6527–6560–6683. The wavelengths of the diffuse interstellar bands marked in Cyg OB2-22B are given by Walborn & Howarth (2000).

absolute visual magnitude,⁷ mass in M_{\odot} ,⁸ the original resolution in Å, the S/N per resolution element, and the reference to the spectroscopic data displayed here. Other key references, including the original sources of the O3 classifications, are given in notes to the table.

It will be noted that new spectral types have been introduced, and a number of the former O3 stars reclassified into

them, in Table 1 and Figures 3–8. These developments have resulted from the detailed consideration of the spectra in this section, and they are described in the following section.

To support a census, all additional stars classified as O3 giants or supergiants in the literature known to us are listed in Table 2. Some of these cases involve data of lower quality or not readily available, spectral peculiarities, or possible membership in “adjacent” subcategories. These last comprise the intermediate O3 If*/WN-A subclass, O3 V or O3 V((f)) types (although the original Carina Nebula representatives are included in Table 1 for reference in the discussion of classification issues), and O4 giants or supergiants in which weaker N IV, N V features are seen in high-quality data. In general, these subcategories will not be considered explicitly here, although some specific cases will be referenced in the context of the discussion.

3.2.1. Supergiant Spectra, Figure 3

The six spectra shown in Figure 3 are placed in the supergiant class because of their strong He II λ 4686 emission features. The strong, narrow N IV λ 4058 emission and N V λ 4604, 4620 absorption lines are further attributes of this spectral type.

⁷ M_V is derived from the photometry and distance modulus, with the assumptions of $(B-V)_0 = -0.32$ and $R = 3.0$ (4.0 for NGC 2244 only), except that in cases with $B-V > 1.00$, E_{B-V} has been calculated from the 50,000 K, $\log g = 5.0$ model of Lejeune, Cuisinier, & Buser (1997) to account for bandpass effects in the BV filters, kindly done by J. Maíz-Apelániz. The calculated E_{B-V} values are 1.94 for Cyg OB2-7 and Pismis 24-1, 2.70 for Cyg OB2-22, 1.99 for Pismis 24-17, and 1.54 for the NGC 3603 stars.

⁸ The first value is from the evolutionary calibration of Vacca et al. (1996) for the corresponding O3–O5 luminosity class, scaled linearly by visual luminosity as may be appropriate for stars with the same T_{eff} and g . The second value has been either interpolated from the models of Schaller et al. (1992) or Schaerer et al. (1993) for the appropriate galaxy, with $\log T_{\text{eff}} = 4.705$ and $BC = -4.5$ and -4.3 for spectral types O2–O3.5 III-I and O3.5–O5 V, respectively, or extrapolated by second-order fits to zero-age main-sequence (ZAMS) mass- M_{bol} relations from the same models for $M > 120 M_{\odot}$.

TABLE 2
OTHER SPECTRA CLASSIFIED AS OR RELATED TO O3f*

Stars	Spectral Types	References	Comments
LH 81/W28-23	O3 V((f))	1	Here O4 III(f+)
LH 90/ST 2-22	O3 III(f*), O3 V((f))	1, 2, 3	Here O4 III(f+)
LH 99/ST 1-71	O3 III(f)	2, 4	Possibly O3 V((f*)), better data needed
LH 101/ST 5-31	O3 If, O3 If*	1, 5	Peculiar, weak lines
LH 101/ST 5-52	O3 V, ON5.5 V((f))	1, 5	Here O3 V((f*)) + OB
LH 117-11/214	O3–O4 III	6, 7, 8	
LH 117-43A/140	O3 III(f*), O3–O4(f*)	7, 8	
P1423	O3–O4 III(f)	9	Better data needed
P1350/H96-28	O3 III(f*)	10	
MH 16	O3 If*	10	Peculiar, weak lines
MH 18, MH 23, MH 24, MH 37, MH 38, MH 41, MH 47, MH 48, MH 57, MH 58, MH 59	O3 III(f*)	10	
MJ 257	O3–O4 If	11	
NGC 3603/HST-22	O3 V((f*))?	4	Possibly, better data needed

REFERENCES.—(1) Massey et al. 2000. (2) Schild & Testor 1992. (3) Testor, Schild, & Lortet 1993. (4) Moffat et al. 2002. (5) Testor & Niemela 1998. (6) Conti et al. 1986. (7) Garmany & Walborn 1987. (8) Massey et al. 1989a. (9) Walborn & Blades 1997. (10) Massey & Hunter 1998. (11) Massey & Johnson 1993.

HD 93129A in Trumpler 14, one of the ionizing clusters of the Carina Nebula (NGC 3372), is the prototype of the subcategory, originally described as such by Walborn (1971a); the relationship of this new kind of spectrum to O4 If+ and WN-A (or WNL) spectra was discussed there and by Walborn (1973b, 1974, 1982) and Walborn et al. (1992).

Cyg OB2-7 was the second O3 supergiant to be found (Walborn 1973c), while Cyg OB2-22A is announced as such here (§ 3.1). These two spectra are of somewhat lower ionization than that of HD 93129A, in terms of their N IV/N III emission-line ratios, an important point to the subsequent discussion.

Pismis 24-1, belonging to the cluster associated with the Galactic nebula NGC 6357, was recently classified by Massey, DeGioia-Eastwood, & Waterhouse (2001); it has an even smaller N IV/N III ratio, barely qualifying for the f* designation, and a weak but definite He I λ 4471 absorption line is detected, yet the ionization ratios are too high and the N V absorption lines too strong for type O4 (Walborn et al. 1995; Walborn & Howarth 2000). This kind of spectrum is well described by a new O3.5 subclass, as will be further discussed later.

MACHO 05:34:41.3–69:31:39 (Ostrov 2001) is a short-period eclipsing binary some distance to the southwest of 30 Doradus. MH 36 (Massey & Hunter 1998) is only 0.4 pc in projection from the center of R136.

All of these spectra have heretofore received the same classification, but their diversity in detail is also noteworthy and likely of physical significance. Ionization differences have already been noted, but the range of λ 4686 profiles is also remarkable: none of the others are exactly like HD 93129A! Cyg OB2-22A and Pismis 24-1 have quite similar, well-defined P Cygni profiles in that line (which rarely occur in Of and WN spectra), and Cyg OB2-7 has a related profile. On the other hand, the greater width of λ 4686 in the MACHO object and MH 36 indicates that they are further along toward the O3 If*/WN-A state (Walborn 1982; Melnick 1985; Walborn et al. 1992; Walborn & Blades 1997; Massey & Hunter 1998). This point may be related to the surprisingly low luminosities and masses of these last two objects, as will also be further discussed later.

3.2.2. Giant Spectra, Figures 4 and 5

Three subcategories of O2–O3 giant spectra are distinguished in Figures 4 and 5. An important result of this study is the recognition that the majority of O2–O3 III(f*) spectra display incipient P Cygni profiles at He II λ 4686 (Fig. 4). Ironically, the prototype and the second known member of the class (HDE 269810 in the LMC [Walborn 1982] and NGC 346-3 in the Small Magellanic Cloud [SMC; Walborn & Blades 1986], respectively; top of Fig. 5) have pure absorption in that line, at least in the data shown here, although the line appears asymmetric in the sense expected from a wind. LH 10-3061 in N11 also has an He II λ 4686 absorption line in the present observation, but the lower resolution spectrogram of Parker et al. (1992) has an apparent, incipient P Cygni profile there. Moreover, an even higher quality digital observation of HDE 269810 by D. J. L. (unpublished) shows a definite incipient P Cygni profile at λ 4686; Walborn (1977) originally classified this spectrum photographically as O3 If* for the identical reason, but Walborn (1982) found pure absorption at that line in a higher quality spectrogram, then preferring the giant luminosity class. Evidence for variable emission features in HD 93129A was cited by Walborn (1971a). Thus, line profile variability in these types of spectra may not be uncommon and should be investigated systematically. Comparing Figures 3–5, one sees that O2–O3 giant and supergiant spectra show a *continuum* of He II λ 4686 profiles from pure (asymmetric) absorption, through P Cygni profiles of different degrees of development, to pure emission. This fact may be related to the result that λ 4686 emission correlates poorly with luminosity in O2–O3 spectra, unlike at later O types where P Cygni profiles are very seldom encountered in this line. It appears that at spectral types O2–O3, He II λ 4686 may be providing primarily information about wind development and/or evolutionary stage, rather than luminosity. The evidence for variability is also suggestive; these stars are likely to be relatively near to the WN stage.

Sk –68°137 was classified O3–O4 III by Conti, Garmany, & Massey (1986), and the earlier type was confirmed by

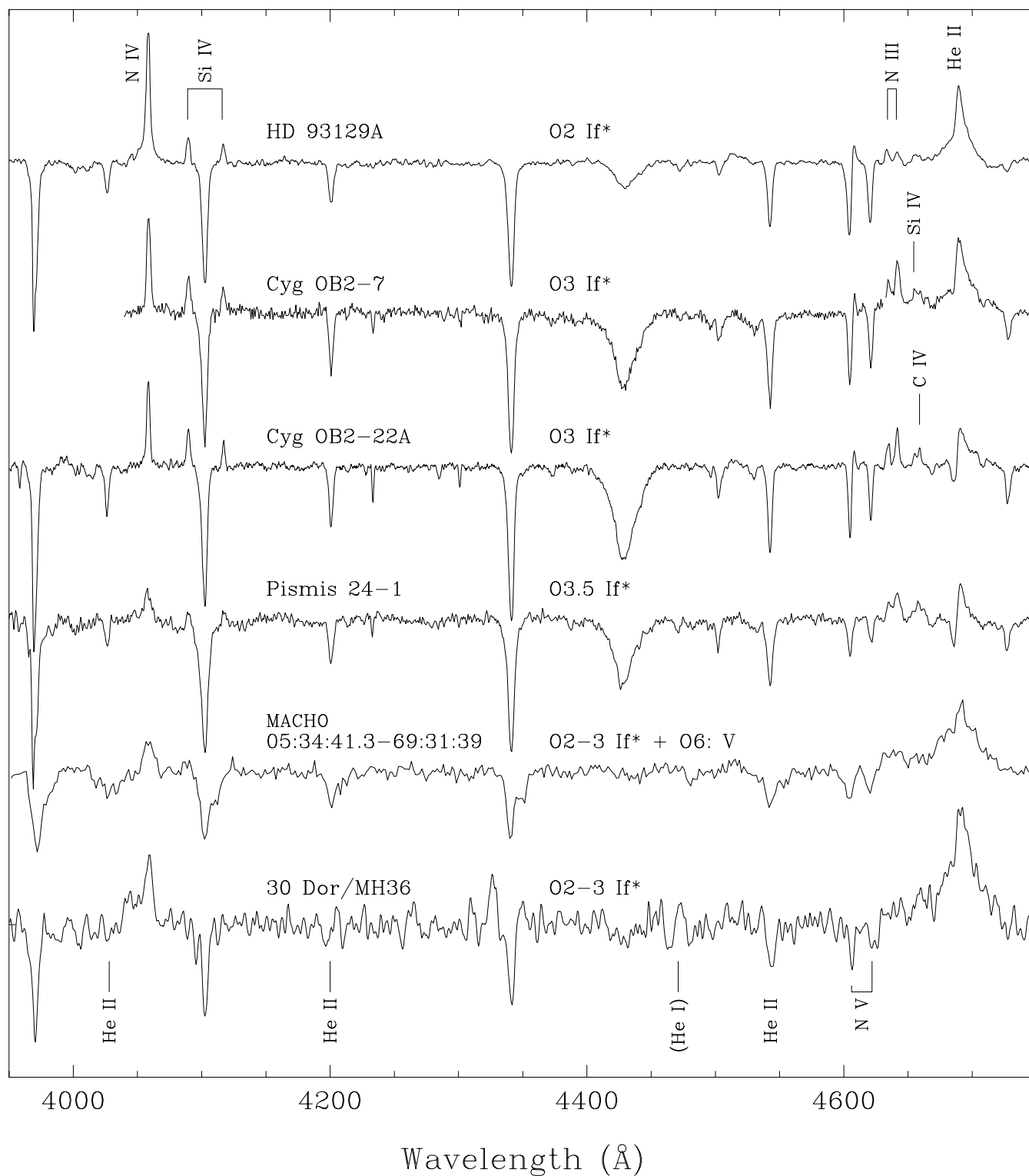


FIG. 3.—Rectified linear-intensity, blue-violet spectrograms of O2–O3 If* stars. In Figs. 3–8, the spectrograms are separated by 0.3 continuum units. The lines identified in the spectrum of HD 93129A are N IV λ 4058; Si IV λ 4089–4116; N III λ 4634–4640–4642; and He II λ 4686. In addition, Si IV λ 4654 is identified in Cyg OB2-7 and C IV λ 4658 in Cyg OB2-22A. The lines identified in MH 36 are He II λ 4026, 4200, 4541; He I λ 4471; and N V λ 4604–4620.

Garmány & Walborn (1987); note that the emission line at 4631 Å is due to Si IV (with possible contributions from N IV, O IV, and S IV) and *not* N III, while C IV λ 4658 is very strong, blended with Si IV λ 4654. These same emission lines are present in the spectrum of HDE 269810 (Fig. 5). Sk $-68^{\circ}137$ is located at the northern edge of the 30 Dora-

lus Nebula, about 200 pc from R136 in projection, and one wonders if it might be a runaway star from the ionizing cluster; a transverse velocity of 100 km s $^{-1}$ would carry it that far in 2 Myr.

LH 64-16 was found to be of spectral type O3 by Massey et al. (2000); although partly a resolution effect, the N IV and

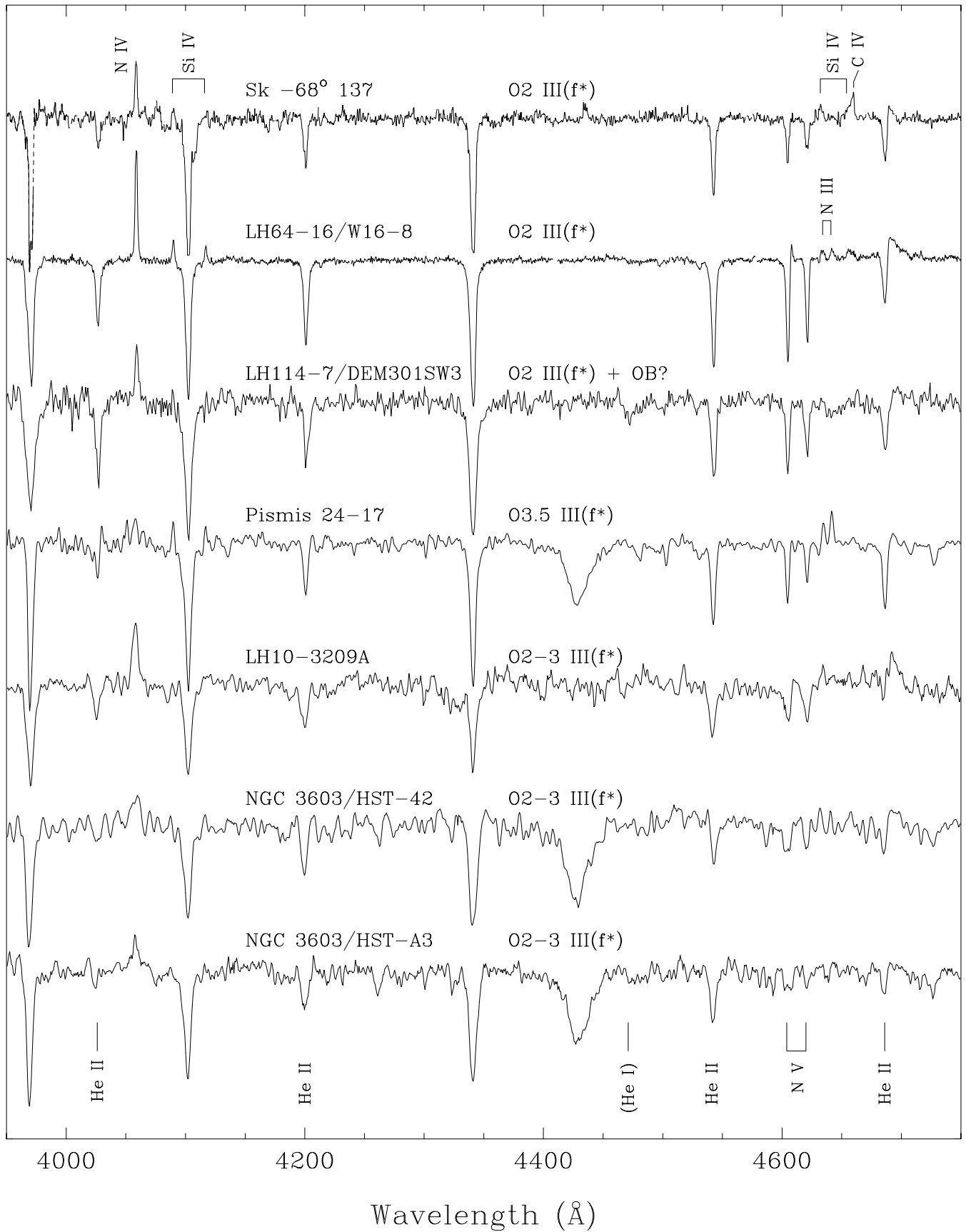


FIG. 4.—Blue-violet spectrograms of O2-O3.5 III(f*) stars with incipient P Cygni profiles at He II $\lambda 4686$. The line identifications are as in Fig. 3, with the addition of Si IV $\lambda 4631$ in Sk -68° 137.

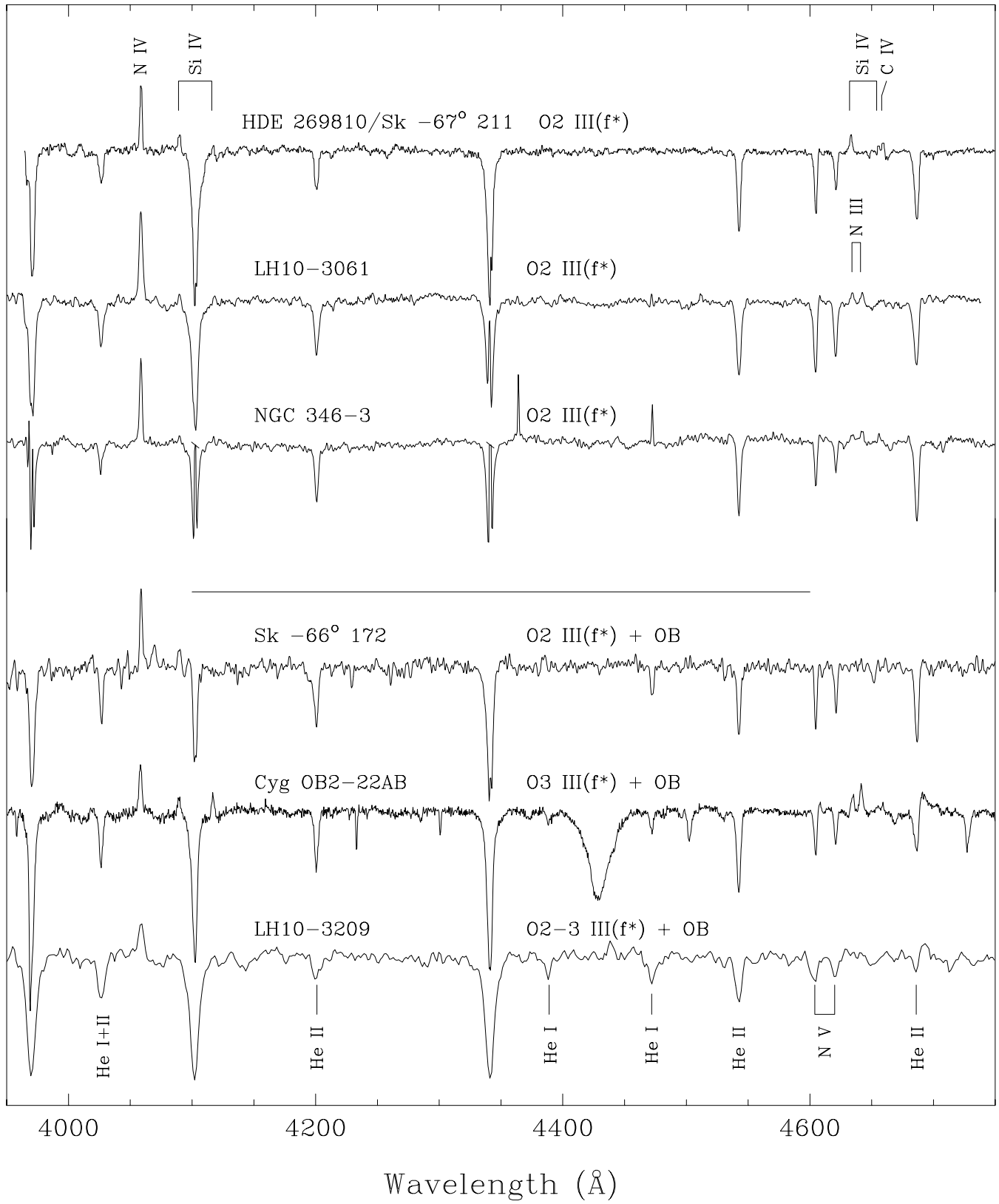


FIG. 5.—Blue-violet spectrograms of three O2 III(f*) stars with pure absorption at He II λ 4686 (*top*) and three O2–O3 III(f*)+OB composite systems (*bottom*). The lines identified are as in the preceding figures, with the addition of He I λ 4026, 4387 in LH 10-3209.

N v lines are remarkably strong in this spectrum, and there is no trace of He I $\lambda 4471$ at very high S/N.

LH 114-7 was classified as O3 by Massey et al. (1995; their No. lmc2-675) and Oey (1996; her No. D301SW-3); there are weak He I lines in this spectrum, more clearly seen in the data of Massey et al. (1995), that likely arise in a companion.

Pismis 24-17 was first classified as O3 by Massey et al. (2001). It shares a small N IV/N III emission ratio with Pismis 24-1 (Fig. 3), but no He I $\lambda 4471$ is detected (there is an artifact just longward of that wavelength), and the N v absorption is far too strong for type O4.

The last three spectrograms in Figure 4 have relatively low spectral resolution by the Faint Object Spectrograph (FOS) on the *Hubble Space Telescope* (*HST*), but the high spatial resolution of *HST* was essential to isolate them within their very compact clusters (see references in Table 1 and further discussion of LH 10-3209 below). NGC 3603 is the most luminous, optically visible H II region in the Galaxy, with strong similarities to 30 Doradus, as well as between the NGC 3603 central cluster and the 30 Doradus cluster core, R136 (Walborn 1973d; Moffat, Drissen, & Shara 1994); the NGC 3603 objects shown here established a close connection between O3 III(f*) and high-luminosity WNL stars (Drissen et al. 1995).

The three spectra at the bottom of Figure 5 combine strong O2–O3 signatures of N IV, N v with moderately strong He I lines, which suggests a composite O2–O3 plus later OB-type system.

The composite nature of Cyg OB2-22 has been demonstrated here (§ 3.1 and Figs. 1 and 2). Note that the composite spectrum has been given a luminosity class of III, but the resolved spectrum of No. 22A a class of I, because of the dilution of the O3 features in the former.

A composite classification of LH 10-3209 in N11B was given by Parker et al. (1992) and Walborn & Parker (1992). This interpretation was subsequently verified directly by *HST* images and spatially resolved spectroscopy, which showed that the He I originates in several close companions to the O3 star (Walborn et al. 1999); the uncontaminated O2–O3 spectrum of LH 10-3209A is reproduced here in Figure 4.

The spectrum of Sk $-66^{\circ}172$ was discussed by Walborn et al. (1995). A faint companion was detected in *HST* images by Kudritzki et al. (1996), and there is evidence from current analysis of scans with an *HST* Fine Guidance Sensor interferometer for further structure in one of the components (E. Nelan 2001, private communication).

Two other cases of O2–O3 spectra with weaker He I lines are included in the previous figures (Pismis 24-1 and LH 114-7), and some further examples will be shown in the subsequent figures. However, in the case of *weak* He I lines detected in high-quality data, a composite interpretation may not be obvious. This general issue will be further discussed later.

3.2.3. Dwarf Spectra, Figure 6

The spectrum of HD 64568 in NGC 2467/Puppis OB2 was the first to be classified as O3 V((f*)), that is, as a dwarf from the strong He II $\lambda 4686$ absorption, but with (weak) N IV $\lambda 4058$ emission stronger than N III $\lambda \lambda 4634, 4640-4642$ (Walborn 1982). Commensurate N v $\lambda \lambda 4604, 4620$ absorption lines are also present. The spectrum of LH 10-3058 in

N11B is very similar and was the second to be so classified (Parker et al. 1992; Walborn & Parker 1992). Both of these spectra show weak but definite He I lines in the present high-quality data (although some uncertainty is introduced by the nebular emission-line subtraction in LH 10-3058). The presence of a later type companion cannot be excluded, but neither can it be assumed from the available information, especially in view of the absolute visual magnitudes of these stars, which are at the faint end of the range for class V (Table 1). As reviewed in § 1, the original definition of spectral class O3 was the absence of He I in the moderate-resolution photographic data then in use. Clearly, the criteria must evolve for data of the quality shown here; these two spectra cannot be classified into any other existing category. Again, the general problem of He I in O2–O3 spectra will be further discussed below.

In contrast, the spectrum of BI 253, first classified as O3 by Massey et al. (1995), shows no hint of He I; note that unlike the previous two, it has no trace of N III emission, either, but does have well-marked C IV $\lambda 4658$ emission, indicating a hotter spectrum, a point that will be taken up later. This star is located at the northwestern edge of the 30 Doradus Nebula (Brunet et al. 1975), about 110 pc from R136 in projection and not far from Sk $-68^{\circ}137$ discussed in the previous section, again suggesting the possibility of a runaway star from the ionizing cluster; in this case a transverse velocity of 55 km s^{-1} would be required for a lifetime of 2 Myr.

Sk $-71^{\circ}51$ is the brightest star in the central cluster of the small, isolated H II region NGC 2103 within Henize N214 south of 30 Doradus (Garmann & Walborn 1987; Walborn 1994); in this case the excessively bright absolute magnitude is clearly due to the aperture photometry of Isserstedt (1975) having included the entire cluster core. There is a strange, semistellar object brighter than the O3 star at the northern edge of this H II region, which may be related to an early epoch of massive star formation; a detailed study of this region will likely prove worthwhile.

The last three stars in Figure 6 belong to the 30 Doradus ionizing cluster and were originally classified as O3 by Melnick (1985) or Walborn & Blades (1997); the stellar designations are from Parker (1993). They are strongly affected by nebular emission lines, but the O2–O3 signatures of N IV, N v are clear. Note that the spectrum of P871 has no N III emission, while the other two do; in these spectra it is unclear whether $\lambda 4658$ is due to C IV or to nebular [Fe III].

3.2.4. Carina Nebula Dwarf Spectra, Figures 7 and 8

Although spectra without the f* (N IV > N III emission) qualifier are not within the purview of this study per se, new, high-quality digital observations of the original O3 V stars in the Carina Nebula (Walborn 1971a, 1973b) are displayed in Figures 7 and 8, for comparison with the spectra in Figure 6 and to support the discussion of classification issues in the next section. The O5 V((f)) spectrum of HD 93204 in the same region is also shown in Figure 7, and those of the primary classification standards HD 46223, O4 V((f+)) and HD 46150, O5 V((f)) in NGC 2244 are shown in Figure 8; these comparison stars were observed during the same runs and with the same equipment as the other stars in their respective figures. All of these spectra now receive the ((f)) or ((f+)) designation, since N III emission is detected; the “+” qualifier denotes the additional presence of Si IV

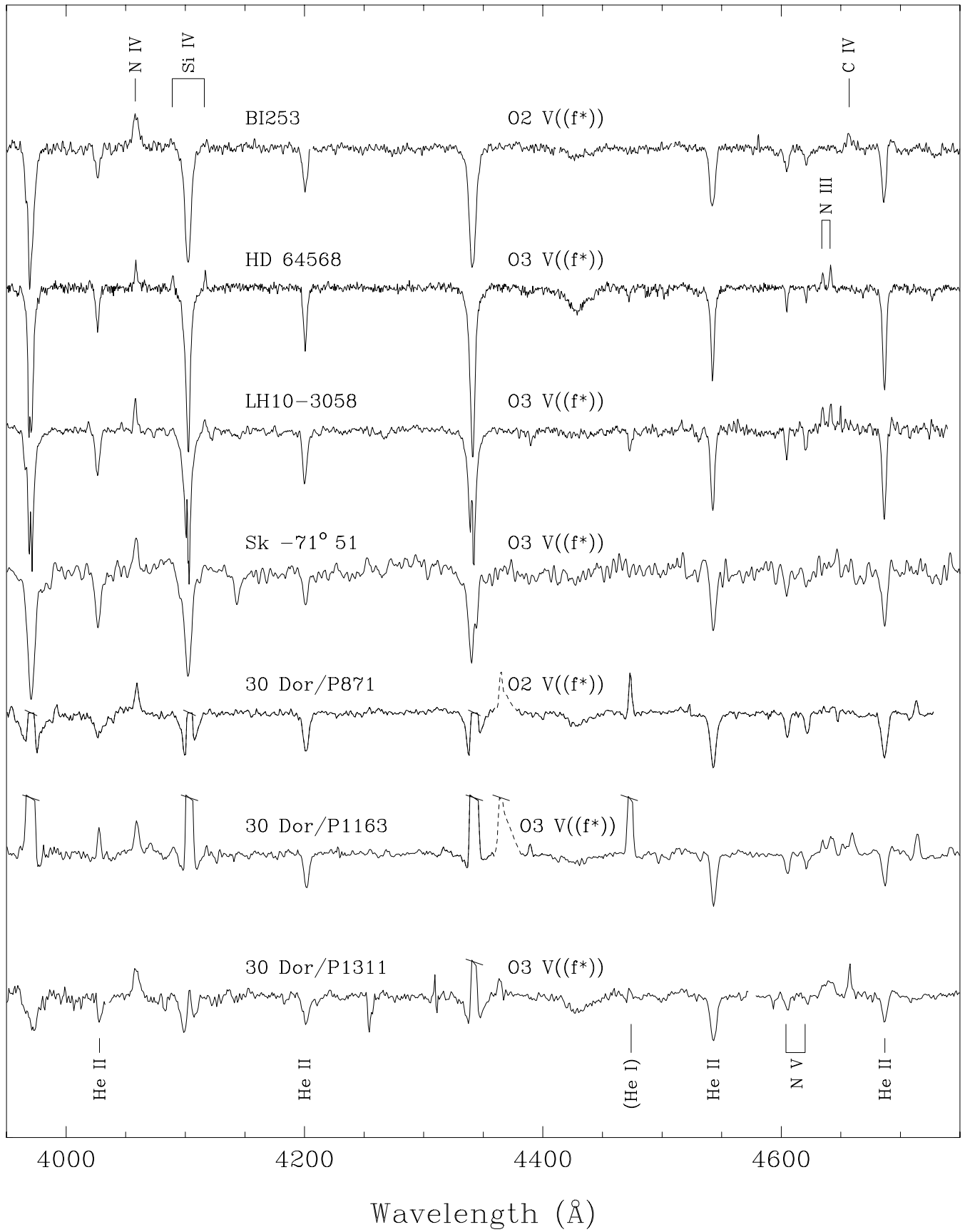


FIG. 6.—Blue-violet spectrograms of O2–O3 V((f*)) stars. The wavelengths of the lines identified are given in the captions of the preceding figures. A number of nebular emission lines have been truncated in the three 30 Doradus objects at the bottom.

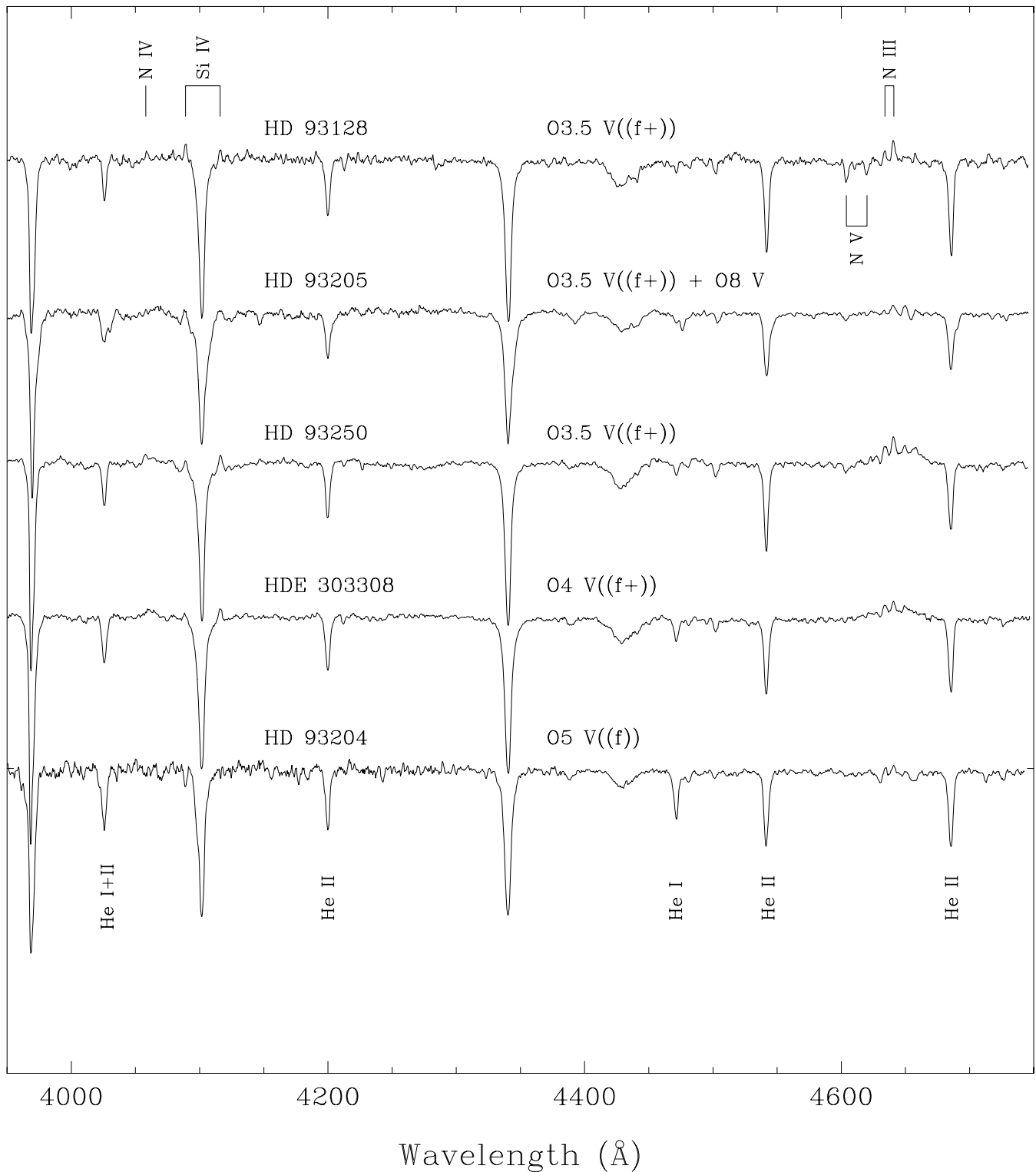


FIG. 7.—ESO NTT/EMMI spectrograms of four original O3 V stars in the Carina Nebula; revised spectral types are shown and the spectrum of an associated O5 V((f)) star is included. The wavelengths of the lines identified are given in the captions of the preceding figures.

$\lambda\lambda 4089, 4116$ emission lines. Weak N IV $\lambda 4058$ emission also appears to be detected in HD 93128, HD 93129B, and HD 93250, but in no case is it as strong as the N III; the N V absorption lines are also clear in these spectra. The strengths of the He I $\lambda 4471$ absorption lines in these data are particularly significant, and the montages are ordered by that fea-

ture. It is clearly detected in all of them, but very weakly in HD 93128, HD 93129B, HD 93205, and HD 93250, consistent with the original O3 classifications (HD 93205 is a double-lined spectroscopic binary with both components visible here, the stronger He I line corresponding to the later type companion; Conti & Walborn 1976; Morrell et al. 2001).

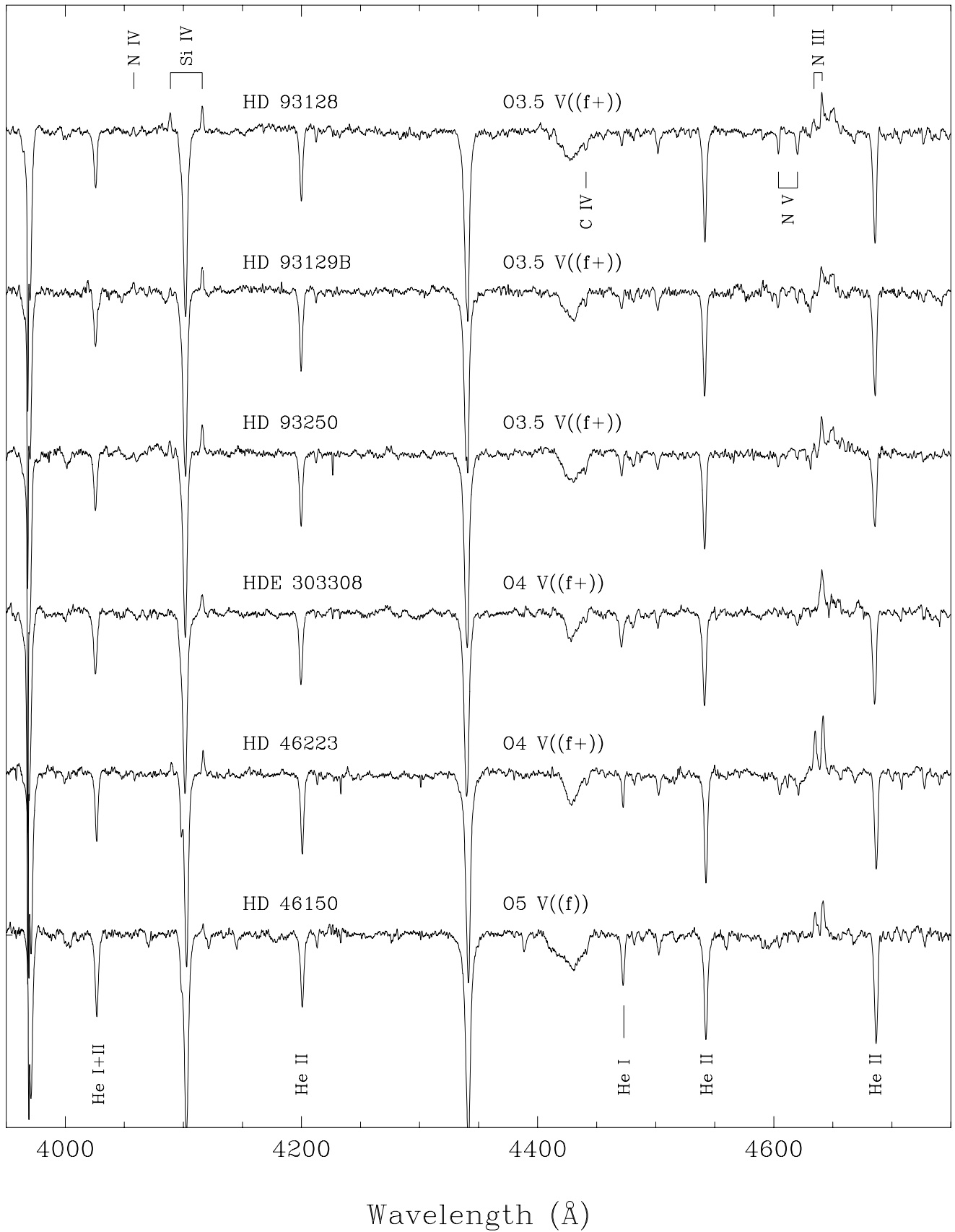


FIG. 8.—CTIO 1.5 m/BME spectrograms of four original O3 V stars in the Carina Nebula; revised spectral types are shown and the spectra of the primary classification standards HD 46223 and HD 46150 in NGC 2244 are included. Some instrumental signatures of these echelle data remain in the profiles of broad or complex features such as interstellar $\lambda 4430$ and the $\lambda\lambda 4630$ – 4650 region, respectively. The wavelengths of the lines identified are given in the captions of the preceding figures, with the addition of C IV $\lambda 4441$ in HD 93128.

However, the He I $\lambda 4471$ /He II $\lambda 4541$ ratio in HDE 303308 requires a reclassification to O4 V((f+)), as clearly shown by the comparison with HD 46223. On the assumption that the spectrum has not changed, the likely explanation is that contamination by the He I nebular emission line affected the original photographic spectrograms of HDE 303308 to a greater extent than was appreciated at the time. In any event, a comparison of HD 93128, HD 93129B, HD 93205, and HD 93250 with HD 64568 and LH 10-3058 in Figure 6 immediately shows another classification issue: while both groups have weak He I lines in data of the present quality, the latter two stars have much larger N IV/N III emission-line ratios, rendering them uncomfortable spectral classmates of the Carina Nebula dwarfs. Finally, note the somewhat weakened He II $\lambda 4686$ absorption line in HD 93250 relative to the other spectra; this effect is in the sense expected for its anomalously bright absolute magnitude (Table 1).

3.2.5. Censur

Table 2 lists additional stars that have been reliably classified as O3 giants or supergiants in the literature, or as O3 V((f*)) or related subcategories. There are 23 stars in Table 2, but two have been reclassified as O4 III(f+) in the present study, leaving 21 stars to be added to the 24 listed in Table 1 (again, not including the Carina Nebula dwarfs). Thus, a total of 45 stars have been classified to date into the O3 subcategories primarily addressed by this study.

Several stars in Table 2 warrant special mention. High-quality data for the two reclassified as O4 III(f+), W28-23 in LH 81 and ST 2-22 in LH 90, are illustrated by Massey et al. (2000); these are the best published examples of this spectral type as defined in the present analysis. Two other objects in Table 2, ST 5-31 in LH 101 also shown by Massey et al. (2000) and MH 16 in 30 Doradus shown by Massey & Hunter (1998), define a new peculiar category in which all line ratios are consistent with type O3 If*, but all lines, both absorption and emission, are anomalously weak. Finally, a composite O3 V((f*))+OB interpretation of the interesting spectrum of ST 5-52 in LH 101, also well illustrated by Massey et al. (2000), is preferred in the present analysis.

The locations of these 45 stars are interesting. As previously mentioned, only two of them, the pair in Cyg OB2, are in the northern hemisphere. Just one, NGC 346-3 (Walborn & Blades 1986; Niemela, Marraco, & Cabanne 1986), is in the SMC; NGC 346 is the largest H II region of the SMC and contains over half the O stars known in that galaxy (Massey, Parker, & Garmany 1989b, in which this star is No. 355). No fewer than 34 of these stars are located in the LMC, and 20 of those are associated with the 30 Doradus ionizing cluster (including the two at the edge of the nebula, Sk $-68^\circ 137$ and BI 253, suggested as possible runaways above). These statistics reemphasize the importance of the LMC, and of 30 Doradus in particular, to the study of the evolution of the most massive stars (Massey & Hunter 1998). The remaining eight stars are located in the southern Milky Way.

4. DISCUSSION

4.1. Spectral Classification Issues

In the detailed consideration of the spectra above, some issues regarding their classification became apparent. Par-

ticularly, ranges in the criteria within a given subcategory, and the presence of weak He I lines in some spectra, require further discussion. Although some of these issues were recognized previously (Walborn 1994), the higher quality and larger sample of present spectroscopic data for the former O3 class now support some revisions and extensions of the classification system.

4.1.1. New Spectral Types O2 and O3.5

The original primary criterion for spectral type O3 was the absence of He I $\lambda 4471$ in moderate-dispersion, photographic spectrograms. Thus, the class was bounded on the low-temperature side only, since the He I/He II classification ratios were no longer available. It might be expected that with improved observational material, a range of (small) He I/He II ratios would be discernible, allowing some lifting of the degeneracy. However, as further discussed in the next section, the presence of weak He I lines in spectra earlier than O4 raises several questions that cannot necessarily be answered by the classification material itself. Thus, it now appears preferable to shift the primary classification criterion to the N IV/N III emission-line ratio in the earliest O-type spectra, which in general correlates well with the He I/He II absorption-line ratio but is not subject to the complications affecting the latter. Following this approach, it has been found useful to introduce new spectral types O2 and O3.5 to describe more consistently the spectra considered here. The criteria and representative stars for the O2–O4 types at the three luminosity classes in use are summarized in Table 3.

Considering first the class V stars in Figures 6–8, one sees very weak He I lines in both the Carina Nebula dwarfs and HD 64568/LH 10-3058, but considerably larger N IV/N III ratios in the latter two spectra. The Carina stars HD 93128, HD 93129B, HD 93205, and HD 93250 are hereby reclassified as O3.5 V((f+)); as previously discussed, HDE 303308 is reclassified to O4 V((f+)). HD 64568 and LH 10-3058 now redefine spectral type O3 V((f*)). Then BI 253, with no trace of N III or He I in its spectrum, becomes the primary standard for the new type O2 V((f*)). Although the data quality is lower, Sk $-71^\circ 51$ remains at O3 V((f*)) for the time being, while P1163 and P1311 definitely belong there as well on the basis of their N III emission-line strengths, despite the strong nebular emission (demonstrating one advantage of the N emission ratio over the He absorption as a classification criterion for these stars). On the other hand, P871 has very weak or no N III emission in its spectrum, thus joining BI 253 at O2 V((f*)).

The O2–O4 N IV/N III scale at luminosity classes I and III is somewhat shifted relative to that at class V, tending toward similar values along diagonal lines in the two-dimensional (spectral type/luminosity class) grid, i.e., entirely analogously to the Of effects at later types (Walborn 1971b). One objective in the reformulation is to minimize revisions to well-established existing classifications. Thus, the small N IV/N III ratios in O4 If+ spectra remain as defined by HD 190429A (Walborn & Howarth 2000) and Sk $-67^\circ 166/167$ (Walborn et al. 1995). The high-quality data for ST 2-22 and W28-23 illustrated by Massey et al. (2000) provide an excellent definition of type O4 III(f+) in the present system. Now the spectra of Pismis 24-1 and 24-17 (Figs. 3 and 4), with N IV \sim N III, define spectral types O3.5 If* and O3.5 III(f*), respectively. HDE 228766

TABLE 3
HORIZONTAL CRITERIA AND STANDARD (EXAMPLE) STARS FOR SPECTRAL TYPES O2–O4

Parameter	O2 If*	O3 If*	O3.5 If*	O4 If+
Criteria	N IV λ 4058 \geq N III λ 4640, no or very weak He I λ 4471	N IV > N III, very weak or no He I	N IV \approx N III, very weak He I	N IV < N III, weak He I
Representative stars	HD 93129A	Cyg OB2-7, Cyg OB2-22A	Pismis 24-1, (HDE 228766), (NGC 2044W-9A), (MH 14)	HD 190429A, Sk -67° 166, Sk -67° 167
Parameter	O2 III(f*)	O3 III(f*)	O3.5 III(f*)	O4 III(f+)
Criteria	N IV λ 4058 \geq N III λ 4640, no or very weak He I λ 4771	N IV > N III, very weak or no He I	N IV \approx N III, very weak He I	N IV < N III, weak He I
Representative stars	HDE 269810, Sk -68° 137, LH 10-3061, LH 64-16, LH 114-7, NGC 346-3, (Sk -66° 172 [+OB])	...	Pismis 24-17	ST 2-22, W28-23
Parameter	O2 V((f*))	O3 V((f*))	O3.5 V((f+))	O4 V((f+))
Criteria	N IV \geq N III, no He I	N IV > or \approx N III, very weak He I	N IV < N III, very weak He I	No N IV, weak He I
Representative stars	BI 253, (P871)	HD 64568, LH 10-3058, (Sk -71° 51), (P1163), (P1311), (ST 5-52 [+OB])	HD 93128, HD 93129B, (HD 93205), (HD 93250)	HD 46223, HDE 303308, W28-5

NOTE.—Representative stars not in parentheses are primary standards; those in parentheses are further examples.

REFERENCES.—HDE 228766: Walborn 1973e. NGC 2044W-9A: Heydari-Malayeri et al. 1993; Walborn et al. 1999. MH 14: Massey & Hunter 1998. HD 190429A: Walborn 1971a; Walborn & Howarth 2000. Sk -67° 166 /167: Walborn et al. 1995. W28-5: Massey et al. 2000. See Table 1 and 2 for other stars.

(Walborn 1973e; see Walborn 1971a for a photographic comparison with HD 190429A), NGC 2044W-9A (Heydari-Malayeri et al. 1993; Walborn et al. 1999; Massey et al. 2000), and MH 14 (Massey & Hunter 1998) are further examples of type O3.5 If*. The spectra of Cyg OB2-7 and 22A (Fig. 3), with N IV > N III, remain to define spectral type O3 If*. All of the previous O3 III(f*) spectra shown here (Figs. 4 and 5) have N IV \geq N III and so move to O2 III(f*), except for those with FOS data (LH 10-3209A and the NGC 3603 stars), which are inadequate to decide and must remain as indeterminate O2–O3 for the present; presumably some O3 III(f*) spectra with N IV/N III ratios similar to those of the Cyg OB2 stars will be found eventually. Finally, HD 93129A (Fig. 3), the original O3 If* spectrum, also has N IV \geq N III and so assumes a new prototype role as the sole current representative of type O2 If*; MH 36 (FOS data) and the MACHO star receive the indeterminate O2–O3 designation for now.

Two methodological or philosophical points should be noted here. (1) The use of an emission-line ratio as a horizontal classification criterion in O-type spectra is a qualitative departure from previous practice, although the strength of the N III emission has been used successfully as a vertical criterion for some time and has even received theoretical support as such (Mihalas, Hummer, & Conti 1972; Mihalas & Hummer 1973). It should be recalled that these are *selective* emission lines (Walborn 2001), which have narrow, symmetrical, and undisplaced profiles quite similar to those of the photospheric absorption lines, and for which there is ample evidence of correlation with the stellar atmospheric parameters. In particular, the correlation of the N IV/N III ratios with the previous O3f*–O4f classifications has been emphasized since the outset and in fact suggested the new system. The full range of these emission-line strengths may

depend on stellar wind effects, but it has also been shown that O-type stellar winds display an excellent correlation with the optical spectral types (Walborn, Nichols-Bohlin, & Panek 1985). Any new classification system remains hypothetical until tested by calibration, application, and modeling. It will be of considerable interest to have detailed investigations of the line formation mechanisms for the N IV and other selective emission lines, comparable to that available for the N III. The effects of metallicity on the N IV/N III should also be taken into account, in view of the results of Crowther (2000). For the moment, there is no indication of a correlation between the new spectral types and the host galaxy, and there are good empirical reasons to propose the emission-line criterion as discussed above. (2) The quality of many of the data discussed here exceeds that of typical classification material, and some developments depend on it, e.g., the detection of Si IV emission in the Carina Nebula dwarfs, as denoted by the ((f+)) notation. The present philosophy is to include all available information in the spectral types, even though some of it may not be reproducible with lower observational quality.

4.1.2. He I in O2–O3 Spectra

The presence of *strong* He I lines in a spectrum with O2–O3 signatures immediately suggests the presence of a later type companion, and this inference has been borne out in three cases discussed in § 3.2.2. ST 5-52, illustrated by Massey et al. (2000), is hypothesized here to be a further case at O3 V((f*))+OB. However, the interpretation of *weak* He I lines in such spectra is not so straightforward, since they may be either intrinsic or from a companion. In the first place, their detection is, of course, a function of observational quality. Kudritzki (1980) and Simon et al. (1983) first

detected weak He I lines in several of the Carina O3 prototypes in high-S/N, high-resolution photographic (IIIa–J) spectrograms, using them to derive physical parameters; Kudritzki et al. (1992) later measured them in high-resolution digital data, and several more cases are clear in the high-S/N data displayed here, as discussed above. In view of the high incidence of spectroscopic binaries and multiple systems among massive stars, the presence of a companion cannot be entirely excluded without intensive radial velocity monitoring and high-resolution imaging. As discussed by Walborn et al. (1999), however, closing the gap between these two techniques in the Magellanic Clouds will require future generations of imaging capabilities. Even the spectroscopic observations are problematic, since they may require very long baselines, large telescopes, and/or high spatial resolution in the case of compact clusters; furthermore, there is always a possibility of an unfavorable inclination. A further problem is He I emission-line contamination from the inhomogeneous nebulae within which many of the hottest stars are found; subtraction uncertainties at moderate resolution can easily produce under- or overestimates of the stellar He I absorption-line strengths.

In several of the spectra discussed here, the weak He I lines detected correlate well with the N IV/N III emission-line ratios and can reasonably be inferred to be intrinsic. Examples are the Carina Nebula dwarfs and Pismis 24-1 at O3.5. Conversely, the absence of He I at very high S/N supports the O2 reclassification of, e.g., BI 253, HDE 269810, and LH 64-16 among others. However, several other cases are less clear or ambiguous. For example, there is a weak He I $\lambda 4471$ line in HD 93129A, but it appears to have a shallow P Cygni profile and may be formed at least partly in the stellar wind (see also Kudritzki et al. 1992); $\lambda 4471$ wind profiles are often present in WN-A spectra, to which that of HD 93129A is related (Walborn 1971a, 1974; Walborn et al. 1992; Walborn & Fitzpatrick 2000). Therefore, given the available information, it has been judged preferable here to shift primary reliance to the N IV/N III emission-line ratio for the horizontal spectral classification of these stars with the present data quality, as discussed in the previous section.

4.1.3. Other Wavelength Ranges

Given the paucity of classification criteria for the hottest spectra in the traditional wavelength range, it is reasonable to hope for additional constraints from other ranges. Such an investigation must, of course, proceed as any classification project involving new parameters, with the observation of a significant sample, charting of the criteria, definition of standards, and a determination of the consistency (or otherwise) with the results from the blue-violet domain. For example, Drissen et al. (1995) found that several N IV and O IV absorption features near 3400 Å discriminated sharply between spectral types O3 and O4. While CNO features must always be viewed with caution as classification criteria, because of the good evidence for mixing of processed material in massive stars (e.g., Walborn et al. 2000 and references therein), a systematic study of the behavior of these near-UV features in as many as possible of the stars discussed here appears well worthwhile. Such a program is being conducted by N. I. M. and N. R. W.

In the case of hot stars the far-UV is likely to provide valuable information, and indeed in an atlas of *IUE* high-reso-

lution data Walborn et al. (1985) found several features that appear to be potential discriminants at the earliest O types. They include O V $\lambda 1371$, in which the presence of a stellar wind profile is a unique signature of O2–O3 giant and supergiant spectra (see also Walborn et al. 1995; Taresch et al. 1997; Haser et al. 1998; de Koter et al. 1998; Herrero et al. 2001); it may also be a useful criterion for dwarf spectra, in ratio to O IV $\lambda\lambda 1339, 1343$ (Morrell et al. 2001). N III $\lambda\lambda 1748, 1752$ appear to strengthen significantly between types O3 and O4 (references cited). Far-UV observations are not yet available for all of the stars discussed here, but a systematic analysis of all existing data and further observations will be worthwhile. Current analyses of the growing *FUSE* database may also provide valuable criteria.

4.2. Absolute Visual Magnitudes

While not a “fundamental” parameter, the derived absolute visual magnitudes are a critical observable, since given a spectral type and an effective temperature calibration, they determine the bolometric luminosities and the masses of the stars. Thus, the M_V values are of vital interest to spectral classifiers, galactic structure specialists, and stellar evolutionists alike. Unfortunately, they are notoriously difficult quantities to obtain for the early-type stars because of uncertainties in their distances, reddening laws, and multiplicities. The first two problems are the most serious in the Galaxy, although the third can be a factor even for quite nearby objects and dominates the other two in the Magellanic Clouds (e.g., Walborn et al. 1999). Other sources of scatter in the luminosity calibration are extraneous physical phenomena that vitiate the normal interpretation of the classification criteria (e.g., in interacting close binaries) and the recently recognized effects of rotation on massive stellar evolution (Heger & Langer 2000; Meynet & Maeder 2000; Maeder & Meynet 2000).

From an analysis of the 10 O3 stars then known, Walborn (1982) concluded that the correlation between the absolute magnitudes and the spectroscopic luminosity classes was considerably poorer than for the later type O stars (e.g., Walborn 1972, 1973a), with large individual discrepancies in both directions and no distinction between classes III and I. The present results extend and confirm the earlier analysis. Inspection of the individual M_V values in Table 1 shows considerable overlap among the luminosity classes. The formal average values are -6.35 ± 0.4 ($n = 6$) for O2–O3.5 If*, -6.0 ± 0.1 ($n = 10$) for O2–O3.5 III(f*), and -5.7 ± 0.2 ($n = 7$) for O2–O3 V((f*)), where standard deviations of the means are quoted. There is a marginal trend in the expected sense, but the differences among the means are within their errors.

This is a disappointing result from the viewpoint of spectral classification, but an important one to know for subsequent astrophysical interpretation of the hottest Population I stars. Several further remarks can be made about some individual cases. MACHO 05:34:41.3–69:31:39 is a 1.4 day eclipsing binary system (Ostrov 2001), a fact that may well be related to its spectroscopic characteristics. Its anomalously faint M_V , as well as that of MH 36 (Massey & Hunter 1998), is reminiscent of the original O3 If*/WN6-A stars Sk $-67^\circ 22$ in the LMC and AB2 in the SMC (Walborn 1982, 1986). A possible hypothesis for further investigation is that all of these faint “supergiant” and “transition” objects may be immediate pre-WN interacting binary sys-

tems. Alternatively, some of them may be pre-WN single stars at the low end of the progenitor mass range, as further discussed in the next section.

In the case of M_V values that are too bright, there is always the possibility of an unresolved multiple system. As already noted above, Sk $-71^\circ 51$ is a demonstrable case in point, the available aperture photometry having included the entire cluster core of NGC 2103. A digital imaging photometric study is required to better resolve the O3 star in this system.

Omitting the three stars just discussed, the average M_V values for the three O2–O3 luminosity classes become -6.95 ± 0.2 ($n = 4$), -6.0 ± 0.1 (no change), and -5.6 ± 0.2 ($n = 6$), a somewhat more satisfying result. The main difference from Walborn (1982) is that the class III mean M_V is now closer to that of class V instead of class I; there was only one class III object in the earlier study (HDE 269810), which is at the bright end of the corresponding M_V range found for 10 stars here.

Of course, there may be other unknown interacting binaries or multiple systems among the remaining discrepant cases in the present sample, but it appears unlikely that such anomalies constitute the entire explanation of the M_V results. Rather, as already mentioned above, the behavior of the primary luminosity criterion He II $\lambda 4686$ is qualitatively different at spectral types O2–O3 from that at later types, suggesting that it may well be sensitive to other competitive effects in addition to luminosity. In particular, the $\lambda 4686$ absorption remains quite strong in the O2–O3 giants, the distinction from the dwarfs being based more on the much greater strengths of the N IV emission and N V absorption features in the giants. Moreover, $\lambda 4686$ tends to develop a P Cygni profile in both giants and supergiants at types O2–O3, which is seldom, or by definition never, observed in *normal* (i.e., typical) O stars at types O4 and later. This distinction in the behavior of He II $\lambda 4686$ at spectral types O2–O3 will be a crucial constraint to be reproduced and explained by astrophysical modeling and interpretation of these extreme stars; it may well turn out to be an evolutionary (and/or rotational?) effect among stars of similar initial (high) masses.

4.3. Masses and Evolutionary Status

There is current controversy regarding the effective temperatures of the O3 stars, and, of course, the new spectral types introduced here remain to be calibrated. Values derived by different authors range from 40,000 (de Koter et al. 1998) to 60,000 K (Puls et al. 1996), with correspondingly large effects on the derived stellar masses (see also Massey & Hunter 1998). Recent line-blanketed models favor lower values (Martins, Schaerer, & Hillier 2002). Here we have adopted the intermediate temperatures near 50,000 K of Vacca, Garmany, & Shull (1996) and made estimates of the evolutionary masses from their calibration; alternatively, we have also made independent estimates from the evolutionary tracks of Schaller et al. (1992) or Schaerer et al. (1993), as explained in footnote 8. These mass estimates are in reasonable agreement with results from detailed evolutionary analyses in the literature (e.g., Puls et al. 1996), except for the very high values for Cyg OB2-22A and Pismis 24-1, which, however, depend sensitively on large model reddening corrections and large extrapolations of the mass calibrations. It should also be noted that some of the few

available orbital mass determinations for the hottest stars tend to give lower values than the evolutionary models (e.g., Ostrov 2001; Morrell et al. 2001), suggesting the possibility of evolutionary mass “inflation,” although Massey, Penny, & Vukovich (2002) find good agreement. The present estimates must suffice for our purposes. Inspection of Table 1 shows a full range of 38–291 M_\odot from the linear scaling, or a somewhat smaller range of 53–210 M_\odot from the evolutionary models, with reasonable agreement inside of the extremes.

How can this large range of masses producing similar spectra be understood? From the outset, it has been clear that the O3 stars are very closely related to type WN, on the basis of both spectral morphology and spatial association. These relationships were clear from the Carina Nebula prototypes (Walborn 1971a, 1973b, 1974), and then in 30 Doradus (Melnick 1985; Walborn & Blades 1997; Massey & Hunter 1998) and NGC 3603 (Drissen et al. 1995). A further striking piece of evidence is the very large N/C abundance ratio in the stellar wind of NGC 346-3 (Walborn et al. 1995, 2000; Haser et al. 1998); it is quite possible that all O2–O3 giants and supergiants have similar large N/C ratios in their winds, but it is obvious only in the SMC object because the low initial systemic abundance allows the very sensitive C IV profile to desaturate. But, there are at least three distinct channels leading to the WN stage: very massive single stars in giant H II regions, post-red supergiants at lower masses, and mass transfer binaries. A reasonable hypothesis from the present empirical information is that all of these diverse WN phenomena may be immediately preceded by an O2–O3 state, leading directly to the large range of masses observed for the latter.

A final observational point that may be either a curious coincidence or a vital clue to the interpretation of the O2–O3 stars is the pairing of very similar spectra in Cyg OB2 and Pismis 24. These two pairs of spectra have details in common (within each pair) that are not shared with any others in the present sample, i.e., these pairs comprise the only giant/supergiant spectra currently classified as O3 or O3.5, respectively, as described above. This circumstance suggests the possibilities of cluster metallicity effects and/or extreme evolutionary synchronization determining the spectroscopic details. It is also reminiscent of the spatial twinning of very rare peculiar objects in the “OB Zoo” reported by Walborn & Fitzpatrick (2000). The derived luminosities and masses within each of the present pairs are quite different, although as noted above the very large values for Cyg OB2-22A and Pismis 24-1 are uncertain. Time will tell the significance or otherwise of this particular point.

5. SUMMARY

We have performed a careful descriptive review of high-quality digital spectroscopic data for a substantial sample of stars previously classified as O3 If*, O3 III(f*), or O3 V((f*)), as well as the O3 V((f)) stars in the Carina Nebula that originally defined the type. A new member of the O3 If* category has been presented, namely, Cyg OB2-22A, which is the second O3 star known in that association and only the second in the northern hemisphere. The principal result of this study is that the previous O3 spectral type has been subdivided into the three new types O2, O3, and O3.5, to accommodate the range in the classification criteria revealed by these data. Thus, a new earliest spectral type has

been defined. Because of various extraneous effects on the detection and interpretation of the very weak or absent He I absorption lines in these spectra, the principal classification criterion has been shifted to the N IV/N III selective emission-line ratio, which was already known to correlate well with the He I/He II absorption-line definition of giant and supergiant types O3 versus O4. All of the Carina Nebula dwarfs have been reclassified as O3.5 V((f+)), except for one, HDE 303308, which has been revised to O4 V((f+)) on the basis of the higher quality data. A census of all previous, pure O3 spectra assigned the f^* parameter (signifying N IV emission stronger than N III) totals 45 stars, of which 34 reside in the LMC and 20 of those in 30 Doradus.

Subject to uncertainties in the distances and reddening corrections of some Galactic stars, and pending the physical calibration of the new spectral types as well as the availability of line-blanketed atmospheric/wind models and (rotating) evolutionary models for masses greater than $120 M_{\odot}$, the absolute visual magnitudes and masses of the O2–O3.5

stars have been reviewed. A major result is that the individual spectral types/luminosity classes show substantially greater ranges in these parameters than is characteristic of the later O classifications or than is reasonably expected from the uncertainties just enumerated. This result may be related to the qualitatively different behavior of the primary luminosity criterion He II $\lambda 4686$ in the O2–O3.5 spectra, namely, the development of P Cygni profiles in that line that are not seen at the later types. A speculative interpretation, supported by both spectral and spatial morphological evidence, is that O2–O3.5 stars may represent an immediate pre-WN phase, so that they mimic the wide luminosity and mass ranges of the latter, corresponding to different formation channels.

We are grateful to Ken Freeman for kindly obtaining the important observation of HD 64568 for this discussion and to Jesús Maíz-Apellániz for the model reddening calculations.

REFERENCES

- Brunet, J. P., Imbert, M., Martin, N., Mianes, P., Prévot, L., Rebeiro, E., & Rousseau, J. 1975, *A&AS*, 21, 109
- Conti, P. S., Garmany, C. D., & Massey, P. 1986, *AJ*, 92, 48
- Conti, P. S., Niemela, V. S., & Walborn, N. R. 1979, *ApJ*, 228, 206
- Conti, P. S., & Walborn, N. R. 1976, *ApJ*, 207, 502
- Crowther, P. A. 2000, *A&A*, 356, 191
- de Koter, A., Heap, S. R., & Hubeny, I. 1998, *ApJ*, 509, 879
- Drissen, L., Moffat, A. F. J., Walborn, N. R., & Shara, M. M. 1995, *AJ*, 110, 2235
- Garmany, C. D., & Walborn, N. R. 1987, *PASP*, 99, 240
- Haser, S. M., Pauldrach, A. W. A., Lennon, D. J., Kudritzki, R.-P., Lennon, M., Puls, J., & Voels, S. A. 1998, *A&A*, 330, 285
- Heger, A., & Langer, N. 2000, *ApJ*, 544, 1016
- Herrero, A., Corral, L. J., Villamariz, M. R., & Martín, E. L. 1999, *A&A*, 348, 542
- Herrero, A., Puls, J., Corral, L. J., Kudritzki, R. P., & Villamariz, M. R. 2001, *A&A*, 366, 623
- Herrero, A., Puls, J., & Villamariz, M. R. 2000, *A&A*, 354, 193
- Heydari-Malayeri, M., Grebel, E. K., Melnick, J., & Jorda, L. 1993, *A&A*, 278, 11
- Isserstedt, J. 1975, *A&AS*, 19, 259
- Kudritzki, R.-P. 1980, *A&A*, 85, 174
- Kudritzki, R.-P., Cabanne, M. L., Husfeld, D., Niemela, V. S., Groth, H. G., Puls, J., & Herrero, A. 1989, *A&A*, 226, 235
- Kudritzki, R.-P., Hummer, D. G., Pauldrach, A. W. A., Puls, J., Najarro, F., & Imhoff, J. 1992, *A&A*, 257, 655
- Kudritzki, R.-P., Lennon, D. J., Haser, S. M., Puls, J., Pauldrach, A. W. A., Venn, K., & Voels, S. A. 1996, in *Science with the Hubble Space Telescope-II*, ed. P. Benvenuti, F. D. Macchetto, & E. J. Schreier (Baltimore: STScI), 285
- Lejeune, Th., Cuisinier, F., & Buser, R. 1997, *A&AS*, 125, 229
- Lortet, M. C., Testor, G., & Niemela, V. 1984, *A&A*, 140, 24
- Maeder, A., & Meynet, G. 2000, *ARA&A*, 38, 143
- Martins, F., Schaerer, D., & Hillier, D. J. 2002, *A&A*, 382, 999
- Massey, P., DeGioia-Eastwood, K., & Waterhouse, E. 2001, *AJ*, 121, 1050
- Massey, P., Garmany, C. D., Silkey, M., & DeGioia-Eastwood, K. 1989a, *AJ*, 97, 107
- Massey, P., & Hunter, D. A. 1998, *ApJ*, 493, 180
- Massey, P., & Johnson, J. 1993, *AJ*, 105, 980
- Massey, P., Lang, C. C., DeGioia-Eastwood, K., & Garmany, C. D. 1995, *ApJ*, 438, 188
- Massey, P., Parker, J. Wm., & Garmany, C. D. 1989b, *AJ*, 98, 1305
- Massey, P., Penny, L. R., & Vukovich, J. 2002, *ApJ*, 565, 982
- Massey, P., & Thompson, A. B. 1991, *AJ*, 101, 1408
- Massey, P., Waterhouse, E., & DeGioia-Eastwood, K. 2000, *AJ*, 119, 2214
- Melnick, J. 1985, *A&A*, 153, 235
- Meynet, G., & Maeder, A. 2000, *A&A*, 361, 101
- Mihalas, D., & Hummer, D. G. 1973, *ApJ*, 179, 827
- Mihalas, D., Hummer, D. G., & Conti, P. S. 1972, *ApJ*, 175, L99
- Moffat, A. F. J., Drissen, L., & Shara, M. M. 1994, *ApJ*, 436, 183
- Moffat, A. F. J., et al. 2002, in preparation
- Morrell, N. I., et al. 2001, *MNRAS*, 326, 85
- Niemela, V. S., Marraco, H. G., & Cabanne, M. L. 1986, *PASP*, 98, 1133
- Oey, M. S. 1996, *ApJ*, 465, 231
- Ostrov, P. G. 2001, *MNRAS*, 321, L25
- Parker, J. Wm. 1993, *AJ*, 106, 560
- Parker, J. Wm., Garmany, C. D., Massey, P., & Walborn, N. R. 1992, *AJ*, 103, 1205
- Pigulski, A., & Kołaczowski, Z. 1998, *MNRAS*, 298, 753
- Puls, J., et al. 1996, *A&A*, 305, 171
- Schaerer, D., Meynet, G., Maeder, A., & Schaller, G. 1993, *A&AS*, 98, 523
- Schaller, G., Schaerer, D., Meynet, G., & Maeder, A. 1992, *A&AS*, 96, 269
- Schild, H., & Testor, G. 1992, *A&AS*, 92, 729
- Simon, K. P., Jonas, G., Kudritzki, R.-P., & Rahe, J. 1983, *A&A*, 125, 34
- Taresch, G., et al. 1997, *A&A*, 321, 531
- Testor, G., & Niemela, V. 1998, *A&AS*, 130, 527
- Testor, G., Schild, H., & Lortet, M. C. 1993, *A&A*, 280, 426
- Vacca, W. D., Garmany, C. D., & Shull, J. M. 1996, *ApJ*, 460, 914
- Vijapurkar, J., & Drilling, J. S. 1993, *ApJS*, 89, 293
- Walborn, N. R. 1971a, *ApJ*, 167, L31
- . 1971b, *ApJS*, 23, 257
- . 1972, *AJ*, 77, 312
- . 1973a, *AJ*, 78, 1067
- . 1973b, *ApJ*, 179, 517
- . 1973c, *ApJ*, 180, L35
- . 1973d, *ApJ*, 182, L21
- . 1973e, *ApJ*, 186, 611
- . 1974, *ApJ*, 189, 269
- . 1977, *ApJ*, 215, 53
- . 1982, *ApJ*, 254, L15
- . 1986, in *IAU Symp. 116, Luminous Stars and Associations in Galaxies*, ed. C. W. H. de Loore, A. J. Willis, & P. Laskarides (Dordrecht: Reidel), 185
- . 1994, in *ASP Conf. Ser. 60, The MK Process at 50 Years: A Powerful Tool for Astrophysical Insight*, ed. C. J. Corbally, R. O. Gray, & R. F. Garrison (San Francisco: ASP), 84
- . 1995, *Rev. Mexicana Astron. Astrofis. Ser. Conf.*, 2, 51
- . 2001, in *ASP Conf. Ser. 242, Eta Carinae and Other Mysterious Stars: The Hidden Opportunities of Emission Spectroscopy*, ed. T. Gull, S. Johansson, & K. Davidson (San Francisco: ASP), 217
- Walborn, N. R., & Blades, J. C. 1986, *ApJ*, 304, L17
- . 1997, *ApJS*, 112, 457
- Walborn, N. R., Drissen, L., Parker, J. Wm., Saha, A., MacKenty, J. W., & White, R. L. 1999, *AJ*, 118, 1684
- Walborn, N. R., Ebbets, D. C., Parker, J. Wm., Nichols-Bohlin, J., & White, R. L. 1992, *ApJ*, 393, L13
- Walborn, N. R., & Fitzpatrick, E. L. 1990, *PASP*, 102, 379
- . 2000, *PASP*, 112, 50
- Walborn, N. R., & Howarth, I. D. 2000, *PASP*, 112, 1446
- Walborn, N. R., Lennon, D. J., Haser, S. M., Kudritzki, R.-P., & Voels, S. A. 1995, *PASP*, 107, 104
- Walborn, N. R., Lennon, D. J., Heap, S. R., Lindler, D. J., Smith, L. J., Evans, C. J., & Parker, J. Wm. 2000, *PASP*, 112, 1243
- Walborn, N. R., Nichols-Bohlin, J., & Panek, R. J. 1985, *International Ultraviolet Explorer Atlas of O-Type Spectra from 1200 to 1900 Å*, NASA RP 1155
- Walborn, N. R., & Parker, J. Wm. 1992, *ApJ*, 399, L87